

## Low-Lying Structure of $^{50}\text{Ar}$ and the $N = 32$ Subshell Closure

D. Steppenbeck,<sup>1,\*</sup> S. Takeuchi,<sup>2,†</sup> N. Aoi,<sup>3</sup> P. Doornenbal,<sup>2</sup> M. Matsushita,<sup>1</sup> H. Wang,<sup>2</sup> Y. Utsuno,<sup>4</sup> H. Baba,<sup>2</sup> S. Go,<sup>1,‡</sup> J. Lee,<sup>2,§</sup> K. Matsui,<sup>5</sup> S. Michimasa,<sup>1</sup> T. Motobayashi,<sup>2</sup> D. Nishimura,<sup>6</sup> T. Otsuka,<sup>1,5</sup> H. Sakurai,<sup>2,5</sup> Y. Shiga,<sup>7</sup> N. Shimizu,<sup>1</sup> P.-A. Söderström,<sup>2</sup> T. Sumikama,<sup>8,||</sup> R. Taniuchi,<sup>5</sup> J. J. Valiente-Dobón,<sup>9</sup> and K. Yoneda<sup>2</sup>

<sup>1</sup>Center for Nuclear Study, University of Tokyo, Hongo, Bunkyo, Tokyo 113-0033, Japan

<sup>2</sup>RIKEN Nishina Center, 2-1, Hirosawa, Wako, Saitama 351-0198, Japan

<sup>3</sup>Research Center for Nuclear Physics, University of Osaka, Ibaraki, Osaka 567-0047, Japan

<sup>4</sup>Japan Atomic Energy Agency, Tokai, Ibaraki 319-1195, Japan

<sup>5</sup>Department of Physics, University of Tokyo, Hongo, Bunkyo, Tokyo 113-0033, Japan

<sup>6</sup>Department of Physics, Tokyo University of Science, Noda, Chiba 278-8510, Japan

<sup>7</sup>Department of Physics, Rikkyo University, Toshima, Tokyo 171-8501, Japan

<sup>8</sup>Department of Physics, Tohoku University, Sendai, Miyagi 980-8578, Japan

<sup>9</sup>Istituto Nazionale di Fisica Nucleare, Laboratori Nazionali di Legnaro, Legnaro 35020, Italy

(Received 20 April 2015; published 25 June 2015)

The low-lying structure of the neutron-rich nucleus  $^{50}\text{Ar}$  has been investigated at the Radioactive Isotope Beam Factory using in-beam  $\gamma$ -ray spectroscopy with  $^9\text{Be}(^{54}\text{Ca}, ^{50}\text{Ar} + \gamma)X$ ,  $^9\text{Be}(^{55}\text{Sc}, ^{50}\text{Ar} + \gamma)X$ , and  $^9\text{Be}(^{56}\text{Ti}, ^{50}\text{Ar} + \gamma)X$  multinucleon removal reactions at  $\sim 220$  MeV/u. A  $\gamma$ -ray peak at 1178(18) keV is reported and assigned as the transition from the first  $2^+$  state to the  $0^+$  ground state. A weaker, tentative line at 1582(38) keV is suggested as the  $4_1^+ \rightarrow 2_1^+$  transition. The experimental results are compared to large-scale shell-model calculations performed in the *sd*pf model space using the SDPF-MU effective interaction with modifications based on recent experimental data for exotic calcium and potassium isotopes. The modified Hamiltonian provides a satisfactory description of the new experimental results for  $^{50}\text{Ar}$  and, more generally, reproduces the energy systematics of low-lying states in neutron-rich Ar isotopes rather well. The shell-model calculations indicate that the  $N = 32$  subshell gap in  $^{50}\text{Ar}$  is similar in magnitude to those in  $^{52}\text{Ca}$  and  $^{54}\text{Ti}$  and, notably, predict an  $N = 34$  subshell closure in  $^{52}\text{Ar}$  that is larger than the one recently reported in  $^{54}\text{Ca}$ .

DOI: 10.1103/PhysRevLett.114.252501

PACS numbers: 21.60.Cs, 23.20.Lv, 27.40.+z, 29.38.Db

The evolution of nuclear shell structure in exotic, neutron-rich isotopes owing to changes in the standard ordering of proton and neutron single-particle orbitals (SPOs) has provided one of the focal points of studies in the fields of experimental and theoretical nuclear physics over the last few decades. Significant progress has been made on the experimental front owing to recent developments in the production of intense rare isotope beams. The nuclear “magic numbers” indicate large energy gaps between proton or neutron SPOs that result in shells of nucleons—analogueous to shells of electrons in atomic physics—that fill completely when the number of protons or neutrons ( $Z$  and  $N$ , respectively) is equal to 2, 8, 20, 28, 50, or 82 [1,2] in stable and near-stable atomic nuclei. However, some of the familiar magic numbers, listed above, disappear in nuclei with a large imbalance of protons and neutrons, while other new ones are known to present themselves [3–5]. A few noteworthy examples include the weakening of the traditional magic numbers  $N = 20$  in the island of inversion [6] around  $^{32}\text{Mg}$  [7,8], and  $N = 28$  in the well-deformed nucleus  $^{42}\text{Si}$  [9–11]. On

the contrary, a new magic number has been reported at  $N = 16$  in exotic oxygen [12–14], for example.

Nuclei in the neutron-rich *pf* shell, which consists of the proton ( $\pi$ ) and neutron ( $\nu$ )  $p_{3/2}$ - $p_{1/2}$  and  $f_{7/2}$ - $f_{5/2}$  spin-orbit partners, have also contributed significant input to the understanding of nuclear shell evolution over recent years. Measurements of reduced transition probabilities to first excited  $2^+$  states ( $2_1^+$ ) and the energies of  $2_1^+$  states [ $E(2_1^+)$ ] in even-even systems have provided evidence for the onset of a new subshell closure at  $N = 32$  in  $^{52}\text{Ca}$  [15,16],  $^{54}\text{Ti}$  [17,18], and  $^{56}\text{Cr}$  [19,20]. This result was recently confirmed by high-precision mass measurements of exotic calcium isotopes [21], and a similar experiment on  $^{52,53}\text{K}$  [22] revealed that the gap at  $N = 32$  persists below the proton magic number  $Z = 20$ . A large subshell closure was also predicted [23,24] at  $N = 34$  along the Ca and Ti isotopic chains; however, this was not supported by experimental measurements on  $^{56}\text{Ti}$  [18,25]. More recently, evidence has emerged for the onset of a sizable subshell closure at  $N = 34$  in  $^{54}\text{Ca}$  [26], which is similar in magnitude to the  $N = 32$  gap in  $^{52}\text{Ca}$ , and theoretical

calculations have highlighted the importance of three-nucleon forces in describing the energy systematics and nuclear masses along the Ca isotopic chain [21,27–32].

In the framework of tensor-force-driven shell evolution [5,33], the onset of the  $N = 32$  and  $34$  subshell closures is attributed to a reduction in the strength of the attractive proton-neutron monopole interaction between the  $\pi f_{7/2}$  and  $\nu f_{5/2}$  SPOs. Namely, as protons are removed from the  $\pi f_{7/2}$  orbital, the strength of the interaction decreases, causing the  $\nu f_{5/2}$  orbital to become progressively less bound. Accordingly, the  $\nu f_{5/2}$  orbital shifts up in energy relative to the  $\nu p_{3/2}$ - $\nu p_{1/2}$  spin-orbit partners, and sizable energy gaps present themselves at  $N = 32$  and  $34$  as the  $\pi f_{7/2}$  orbital effectively empties approaching  $Z = 20$  (see, for example, Fig. 1 of Ref. [26] for a schematic representation of the development of these neutron subshell gaps).

The Ar isotopes ( $Z = 18$ ) approaching  $N = 32$  have also attracted much attention recently. In  $^{46}\text{Ar}$ , which contains the traditional neutron magic number  $N = 28$ , the enhanced  $E(2_1^+)$  value [34,35] and reduced transition probability,  $B(E2; 0_1^+ \rightarrow 2_1^+) [\equiv B(E2\uparrow)]$ , obtained from intermediate-energy Coulomb excitation reactions [36,37], provide evidence supporting a robust  $N = 28$  shell closure in this nucleus. The preliminary  $B(E2\uparrow)$  result presented in Ref. [38], which was also deduced using Coulomb excitation, is consistent with the two previous reports [36,37] within  $\sim 1\sigma$ . A measurement of the lifetime of the  $2_1^+$  state [39] yielded a larger  $B(E2\uparrow)$  value, although the result is quoted with relatively large uncertainties. Recent relativistic mean-field calculations [40] predict a  $B(E2\uparrow)$  that is consistent with the Coulomb excitation results [36,37]; however, shell-model calculations [41–43] predict much larger values. Based on these results, the question of whether or not  $N = 28$  remains a robust shell closure in Ar isotopes is, therefore, an intriguing one, particularly since  $^{46}\text{Ar}$  lies on the pathway between the doubly magic,

spherical nucleus  $^{48}\text{Ca}$  and  $^{44}\text{S}$ , which exhibits a coexistence of spherical and deformed configurations [44–47]. Very recent mass measurements of  $^{48}\text{Ar}$  and  $^{49}\text{Ar}$  [48] have, however, added an important piece to the puzzle, since the systematics presented for Ar isotopes mirror those of Ca and Ti and, therefore, provide robust evidence for a strong  $N = 28$  shell closure. It is noted that higher-lying excited states in  $^{46}\text{Ar}$  have also been identified [49,50].

The  $N = 30$  isotope,  $^{48}\text{Ar}$ , has also been studied using deep-inelastic transfer reactions [51], heavy-ion-induced nucleon-exchange reactions [52], and Coulomb excitation [43] within the last decade. In Ref. [51], the structure of  $^{48}\text{Ar}$  was discussed in terms of triaxiality owing to characteristic signatures of experimental  $E(4_1^+)/E(2_1^+)$  and  $E(2_2^+)/E(2_1^+)$  energy ratios and a theoretical prediction of a low-lying  $3_1^+$  state, while Ref. [43] focused on the study of quadrupole collectivity established from a measurement of the  $B(E2\uparrow)$  reduced transition probability using intermediate-energy Coulomb excitation. Another noteworthy outcome of Ref. [43] is that the reduced transition probability extracted for the 1227-keV transition in  $^{47}\text{Ar}$  also lies well below shell-model predictions, which mirrors the situation for the  $B(E2\uparrow)$  values deduced for  $^{46}\text{Ar}$  in the earlier Coulomb excitation experiments [36,37]. The novel experimental techniques presented in Ref. [52] confirm the energies of the  $2_1^+$  and  $4_1^+$  states in  $^{48}\text{Ar}$  reported in the previous study [51], in addition to providing the energy of the first  $2^+$  state in  $^{46}\text{S}$ .

In the present Letter, a spectroscopic study of the neutron-rich nucleus  $^{50}\text{Ar}$  is presented. Preliminary results are discussed in Ref. [53]. This is the heaviest Ar isotope to be investigated using  $\gamma$ -ray spectroscopy to date. A decay study of  $^{50}\text{Ar}$  previously reported the lifetime of the ground state to be 85(30) ms [54]. The motivation for the present Letter is related to two main aspects: First, to further examine the character of the  $N = 32$  subshell closure in  $Z < 20$  nuclei on the experimental front, and, second, to enhance our general understanding of the structures of exotic isotopes and the treatment of nuclear shell evolution at extreme neutron-to-proton ratios.

The experiment was performed at the Radioactive Isotope Beam Factory in Japan, operated by the RIKEN Nishina Center and the Center for Nuclear Study, University of Tokyo, using a primary beam of  $^{70}\text{Zn}^{30+}$  ions at 345 MeV/u with a typical intensity of  $\sim 60$  pnA. The projectile fragmentation technique was adopted to generate a fast radioactive beam ( $\sim 220$  MeV/u) that contained the  $N = 34$  isotones  $^{54}\text{Ca}$ ,  $^{55}\text{Sc}$ , and  $^{56}\text{Ti}$ , among other constituents. The particle identification plot for the secondary beam is provided in Refs. [26,53]. The beam constituents were identified on an event-by-event basis using standard techniques (see, for example, Ref. [55] for further details) in which projectile magnetic rigidities ( $B\rho$ ), times of flight ( $T$ ), and energy losses in an ionization

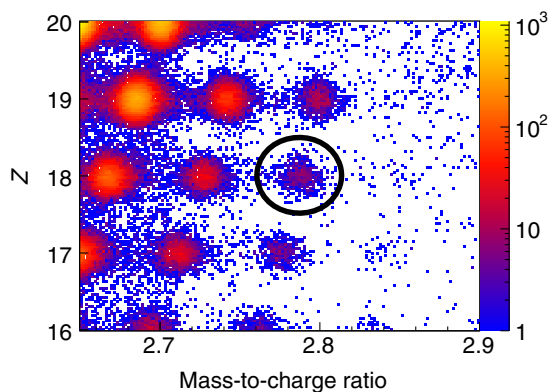


FIG. 1 (color online). Particle identification plot for reaction products measured by the ZDS. Events enclosed by the black circle correspond to  $^{50}\text{Ar}$ . The color scale indicates the number of events per histogram bin.

chamber ( $\Delta E$ ) were measured along the beam line of the BigRIPS separator [56], which was optimized for the transmission of  $^{55}\text{Sc}$ . The typical rates of  $^{54}\text{Ca}$ ,  $^{55}\text{Sc}$ , and  $^{56}\text{Ti}$  transported through BigRIPS were 0.04, 12, and 125 particles per second per pA of primary beam, respectively. The radioactive ion beam was delivered to a 10-mm-thick  $^9\text{Be}$  reaction target at the eighth focal plane along the beam line to induce nucleon removal reactions. The reaction products were identified by the ZeroDegree spectrometer (ZDS) [56] using the same general ( $B\rho-T-\Delta E$ ) techniques as discussed for BigRIPS. Although the ZDS was optimized for the transmission of  $^{54}\text{Ca}$  [26], the  $N = 32$  isotope  $^{50}\text{Ar}$  also fell within the acceptance of the spectrometer, which is indicated in Fig. 1. The reaction target was surrounded by a high-efficiency  $\gamma$ -ray detector array (DALI2) [57] consisting of 186 NaI(Tl) detectors positioned at angles of  $\sim 20^\circ$ – $150^\circ$  relative to the beam line. The array was calibrated using standard  $^{60}\text{Co}$ ,  $^{88}\text{Y}$ , and  $^{137}\text{Cs}$  sources. Data acquisition was triggered by the arrival of an ion at the end of the ZDS measured in coincidence with at least one  $\gamma$  ray in DALI2. Data were accumulated in this way for approximately two days.

The Doppler-corrected  $\gamma$ -ray energy spectrum, deduced from the sum of the  $^9\text{Be}(^{54}\text{Ca}, ^{50}\text{Ar} + \gamma)X$ ,  $^9\text{Be}(^{55}\text{Sc}, ^{50}\text{Ar} + \gamma)X$ , and  $^9\text{Be}(^{56}\text{Ti}, ^{50}\text{Ar} + \gamma)X$  multinucleon removal reactions, is presented in Fig. 2(a); this spectrum contains the sum of all  $\gamma$ -ray multiplicities ( $M_\gamma \geq 1$ ). A histogram containing only  $M_\gamma < 4$  events, which has an improved peak-to-total ratio, is provided in Fig. 2(b) for reference. It is noted that the contribution to the yield of  $^{50}\text{Ar}$  from reactions other than those listed

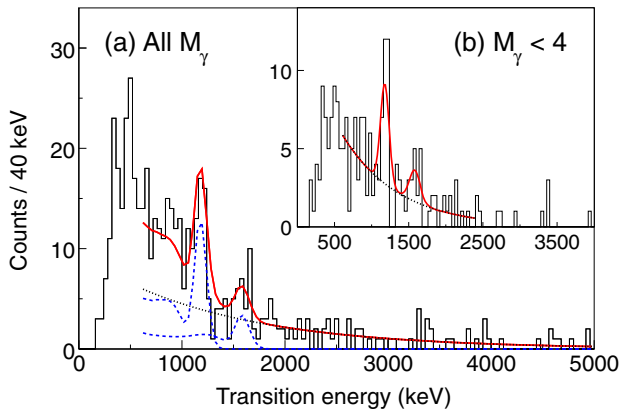


FIG. 2 (color online). Doppler-corrected  $\gamma$ -ray energy spectra for  $^{50}\text{Ar}$  deduced in the present Letter. (a) Spectrum with no  $M_\gamma$  restriction ( $M_\gamma \geq 1$ ). The dashed blue lines are GEANT4 simulated  $\gamma$ -ray response functions. (b) Spectrum with a  $\gamma$ -ray multiplicity selection of  $M_\gamma < 4$ . The solid red line indicates the fit to the data where the widths of the two Gaussian functions have been fixed to simulated values. The dotted black lines are exponential fits to the background in both panels.

above is negligible. The most intense  $\gamma$ -ray peak in the spectrum, the line at 1178(18) keV, is assigned as the transition from the first  $2^+$  state to the  $0^+$  ground state in  $^{50}\text{Ar}$ . A weaker line is also present in the spectrum at 1582 (38) keV, which is suggested to be the  $4_1^+ \rightarrow 2_1^+$  transition (fits to the data were performed using the maximum likelihood method). Statistics were insufficient to confirm the decay scheme through  $\gamma\gamma$  coincidence relationships. The spin-parity assignments are based on the preferential population of yrast states reported in similar reactions (see, for example, Refs. [10,26,58,59]), energy systematics along the Ar isotopic chain [35], and predictions of shell-model calculations, which are discussed below. Errors are statistical, and systematic uncertainties combined in quadrature; the statistical error is dominant for both transitions. The systematic error includes contributions from the  $\gamma$ -ray energy calibration ( $\lesssim 1\%$ ) and possible shifts in  $\gamma$ -ray peak positions owing to uncertainties in the lifetimes of higher-lying excited states that may also have been populated by the reactions. This component of the error was estimated using simulations with the code GEANT4 [60]. Owing to the relatively low number of events in the 1582-keV peak, it is assigned here as a tentative transition; however, it is important to realize that, first, the width of the peak is comparable to the simulated value, which is indicated in Fig. 2, and, second, the efficiency-corrected relative intensity ( $\sim 35\%$  relative to the  $2_1^+ \rightarrow 0_1^+$  transition) is consistent with values measured for  $4_1^+ \rightarrow 2_1^+$  transitions in other reaction channels—for example, the relative intensity of the  $4_1^+ \rightarrow 2_1^+$  transition in  $^{48}\text{Ar}$ , which was also deduced from the data of the present study, is consistent with the value for  $^{50}\text{Ar}$ . However, it is stressed that the 1582-keV peak should be confirmed by a higher-statistics experiment in the future.

The energies of the  $2_1^+$  and  $4_1^+$  states deduced in the present Letter for  $^{50}\text{Ar}$  are presented alongside values for lighter Ar isotopes [35] in Fig. 3. Notably, and in a similar general fashion to measurements along the Ca [15,16], Ti [17,18], and Cr [19,20] isotopic chains, a local rise in  $E(2_1^+)$  is observed at  $N = 32$  relative to the  $N = 30$  even-even neighbor, and is, therefore, suggestive of a persistent  $N = 32$  subshell closure below Ca ( $Z = 20$ ). In order to investigate the nature of the increase in  $E(2_1^+)$  at  $N = 32$  in greater detail, shell-model calculations employing the SDPF-MU effective interaction [11] were performed, which are also displayed in Fig. 3. The calculations adopted full  $sd$  and  $pf$  model spaces for protons and neutrons, respectively, and used effective proton and neutron charges of  $e_\pi = 1.35e$  and  $e_\nu = 0.35e$  in accordance with Ref. [11]. In the present study, the original SDPF-MU Hamiltonian was modified using recent experimental data on exotic Ca [26] and K [61] isotopes; the  $pf$  component of the new interaction is the modified GXPF1B Hamiltonian introduced in Ref. [26], although details of the modifications are provided elsewhere [62,63]. The new calculations, which are indicated by the solid lines in Fig. 3, generally provide a

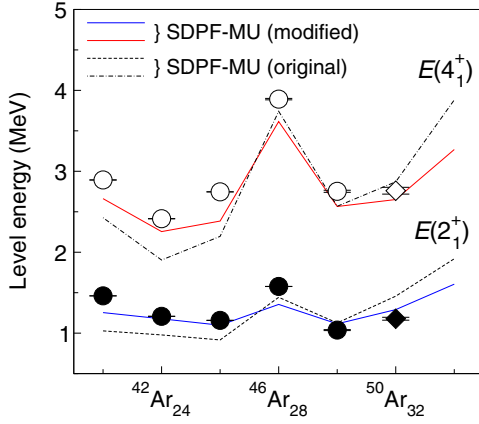


FIG. 3 (color online). Systematics of  $E(2_1^+)$  (filled symbols) and  $E(4_1^+)$  (open symbols) for even-even Ar isotopes [35]. The results of the present Letter are indicated by diamonds at  $N = 32$ . The solid lines are shell-model predictions of  $E(2_1^+)$  (blue) and  $E(4_1^+)$  (red) using the modified SDPF-MU effective interaction, while the dashed lines are predictions of the original SDPF-MU Hamiltonian. Note that the experimental  $2_1^+$  and  $4_1^+$  spin-parity assignments for  $^{48}\text{Ar}$  [35] and  $^{50}\text{Ar}$  (present Letter), and the  $4_1^+$  assignments for  $^{42,44}\text{Ar}$  [35], are tentative.

satisfactory description of the experimental data along the Ar isotopic chain, including the energies deduced in the present Letter for  $^{50}\text{Ar}$ . However, it is noted that the peaks in  $E(2_1^+)$  and  $E(4_1^+)$  at  $N = 28$  are less pronounced in the modified interaction, and the energies fall below the experimental values.

As mentioned above, the rise in  $E(2_1^+)$  is naively suggestive of a sizable  $N = 32$  subshell gap along the Ar isotopic chain. Indeed, the modified SDPF-MU interaction indicates that the magnitude of the  $N = 32$  subshell closure in  $^{50}\text{Ar}$  ( $\sim 2.3$  MeV) is comparable to the  $N = 32$  gaps in  $^{52}\text{Ca}$  and  $^{54}\text{Ti}$  ( $\sim 2.4$  and  $2.5$  MeV, respectively), where the experimental evidence for the  $N = 32$  closure is compelling [15–18,21]. Here, the magnitude of the  $N = 32$  subshell gap is defined as the difference in energy between the  $\nu(p_{3/2}^4)$  and  $\nu(p_{3/2}^3 p_{1/2})$  configurations calculated with the monopole interaction. According to the modified SDPF-MU Hamiltonian, the  $0^+$  ground state and yrast  $2^+$  and  $4^+$  excited states in  $^{50}\text{Ar}$  are all rather mixed. In fact, the largest contributions to the wave function of the  $0^+$  ground state are the  $\pi(d_{5/2}^6 d_{3/2}^2 s_{1/2}^2) - \nu(p_{3/2}^4)$ ,  $\pi(d_{5/2}^6 d_{3/2}^2 s_{1/2}^2) - \nu(p_{3/2}^2 p_{1/2}^2)$ , and  $\pi(d_{5/2}^6 d_{3/2}^4) - \nu(p_{3/2}^4)$  configurations, which contribute 33%, 10%, and 8%, respectively, while all other individual configurations contribute  $\leq 5\%$  to the wave function (these quantities were extracted using the code of Ref. [64]). Moreover, the calculations indicate that the most significant contribution to the first  $2^+$  state is the  $\pi(d_{5/2}^6 d_{3/2}^2 s_{1/2}^2) - \nu(p_{3/2}^3 p_{1/2})$  configuration (16%), while all other configurations contribute  $\leq 7\%$  individually. For the  $4_1^+$  level, the largest

contributions to the wave function are the  $\pi(d_{5/2}^6 d_{3/2}^2 s_{1/2}^2) - \nu(f_{7/2}^{-1} p_{3/2}^4 p_{1/2})$  and  $\pi(d_{5/2}^6 d_{3/2}^3 s_{1/2}) - \nu(p_{3/2}^3 p_{1/2})$  configurations, both with a weight of 16% each, while all other configurations carry values of  $\leq 7\%$  each. In the case of the  $N = 32$  isotope  $^{52}\text{Ca}$ , however, which contains a closed proton core ( $Z = 20$ ), the  $0^+$  ground state and  $2_1^+$  state are dominated ( $\sim 90\%$ ) by the  $\pi(d_{5/2}^6 d_{3/2}^4 s_{1/2}^2) - \nu(p_{3/2}^4)$  and  $\pi(d_{5/2}^6 d_{3/2}^4 s_{1/2}^2) - \nu(p_{3/2}^3 p_{1/2})$  configurations, respectively, indicating that a single neutron excitation across the  $N = 32$  subshell closure ( $\nu p_{3/2} \rightarrow \nu p_{1/2}$ ) is mainly responsible for the first excited  $2^+$  state in  $^{52}\text{Ca}$ . Indeed, the fact that the  $2_1^+$  level is predominantly a neutron excitation has been demonstrated, since the state is not fed directly by the two-proton knockout reaction [16]. This is in contrast to  $^{50}\text{Ar}$  where the wave function is rather mixed and, therefore, the increase in  $E(2_1^+)$  at  $N = 32$  appears to be much less significant along the Ar isotopic chain despite the  $\nu p_{3/2} - \nu p_{1/2}$  energy gaps being similar in magnitude.

In a previous study [65], the strength of the  $\nu p_{3/2} - \nu p_{1/2}$  spin-orbit splitting in  $^{47}\text{Ar}$  was investigated using the  $^{46}\text{Ar}(d, p)^{47}\text{Ar}$  transfer reaction and compared to the value in  $^{49}\text{Ca}$ . A reduction in the magnitude of the  $\nu p_{3/2} - \nu p_{1/2}$  energy gap of  $0.89(12)$  MeV relative to  $^{49}\text{Ca}$  was reported; however, it was later argued [66], based on theoretical corrections owing to fragmentation of the  $p$ -shell spectroscopic strength, that the difference in the  $\nu p_{3/2} - \nu p_{1/2}$  spin-orbit splitting between Ar and Ca is relatively minor. Thus, the conclusion of Refs. [65,66] supports the prediction of the modified Hamiltonian in the present work, which indicates that the difference in the magnitude of the  $p$ -shell spin-orbit splitting between Ar and Ca is rather small ( $\sim 0.1$  MeV).

Although a tentative spin-parity of  $4_1^+$  is assigned to the 2760(42)-keV state in the present Letter, the shell-model calculations predict the  $2_2^+$  state to lie within 50 keV of the yrast  $4^+$  state and, therefore, an assignment of  $J^\pi = 2^+$  for this level cannot be completely ruled out. It is also interesting to note that the shell-model calculations indicate a further increase in  $E(2_1^+)$  along the Ar isotopic chain at  $N = 34$  (see Fig. 3). Indeed, this is intriguing given the recent measurement of a sizable  $N = 34$  subshell closure in exotic Ca isotopes [26]. In fact, the calculations indicate that the magnitude of the  $N = 34$  subshell closure in  $^{50}\text{Ar}$ , assuming a  $\pi d_{3/2}^{-2}$  configuration, is  $\sim 3.1$  MeV, which exceeds the value in  $^{54}\text{Ca}$  ( $\sim 2.6$  MeV). Further details on the evolution of the  $\nu p_{1/2} - \nu f_{5/2}$  energy gap in  $Z < 20$  nuclei are discussed elsewhere [62,63].

In summary, the low-lying structure of the neutron-rich nucleus  $^{50}\text{Ar}$  has been investigated using multinucleon removal reactions from  $^{54}\text{Ca}$ ,  $^{55}\text{Sc}$ , and  $^{56}\text{Ti}$  projectiles at  $\sim 220$  MeV/u. The first  $2^+$  state, deduced in the present Letter using in-beam  $\gamma$ -ray spectroscopy, is reported to lie at

1178(18) keV. A weaker, tentative transition with an energy of 1582(38) keV is suggested to depopulate the first  $4^+$  level at 2760(42) keV. The experimental results are reproduced in a satisfactory manner by shell-model calculations employing a modified SDPF-MU effective interaction [62], which generally provides a systematic improvement to the description of  $E(2_1^+)$  and  $E(4_1^+)$  along the Ar isotopic chain compared to the original Hamiltonian [11]. The calculations indicate that the magnitude of the  $N = 32$  subshell gap in  $^{50}\text{Ar}$  is similar to those in  $^{52}\text{Ca}$  and  $^{54}\text{Ti}$ , where the evidence for the  $N = 32$  subshell closure is well documented [15–18,21]. Interestingly, the shell-model calculations predict a relatively high  $E(2_1^+)$  value for  $^{52}\text{Ar}$  and, therefore, future measurements of excited states in this nucleus are encouraged to test the prediction.

We thank the RIKEN Nishina Center accelerator staff and the BigRIPS team for their contributions to the experiment. This work is part of the CNS-RIKEN joint research project on large-scale nuclear structure calculations. D. S. acknowledges financial support from the Japan Society for the Promotion of Science under Grant No. 26 04327.

\*steppenbeck@riken.jp

Present address: RIKEN Nishina Center, 2-1, Hirosawa, Wako, Saitama 351-0198, Japan.

†Present address: Department of Physics, Tokyo Institute of Technology, Meguro, Tokyo 152-8551, Japan.

‡Present address: Department of Science and Engineering, University of Tennessee, Knoxville, Tennessee 37996-1200, USA.

§Present address: Department of Physics, University of Hong Kong, Pokfulam Road, Hong Kong.

||Present address: RIKEN Nishina Center, 2-1, Hirosawa, Wako, Saitama 351-0198, Japan.

- [1] O. Haxel, J. H. D. Jensen, and H. E. Suess, *Phys. Rev.* **75**, 1766 (1949).
- [2] M. Goeppert Mayer, *Phys. Rev.* **75**, 1969 (1949).
- [3] A. Gade and T. Glasmacher, *Prog. Part. Nucl. Phys.* **60**, 161 (2008).
- [4] O. Sorlin and M.-G. Porquet, *Prog. Part. Nucl. Phys.* **61**, 602 (2008).
- [5] T. Otsuka, *Phys. Scr.* **T152**, 014007 (2013).
- [6] E. K. Warburton, J. A. Becker, and B. A. Brown, *Phys. Rev. C* **41**, 1147 (1990).
- [7] C. Détraz, D. Guillemaud, G. Huber, R. Klapisch, M. Langevin, F. Naulin, C. Thibault, L. C. Carraz, and F. Touchard, *Phys. Rev. C* **19**, 164 (1979).
- [8] T. Motobayashi *et al.*, *Phys. Lett. B* **346**, 9 (1995).
- [9] B. Bastin *et al.*, *Phys. Rev. Lett.* **99**, 022503 (2007).
- [10] S. Takeuchi *et al.*, *Phys. Rev. Lett.* **109**, 182501 (2012).
- [11] Y. Utsuno, T. Otsuka, B. A. Brown, M. Honma, T. Mizusaki, and N. Shimizu, *Phys. Rev. C* **86**, 051301(R) (2012).
- [12] C. R. Hoffman *et al.*, *Phys. Rev. Lett.* **100**, 152502 (2008).
- [13] R. Kanungo *et al.*, *Phys. Rev. Lett.* **102**, 152501 (2009).
- [14] C. R. Hoffman *et al.*, *Phys. Lett. B* **672**, 17 (2009).
- [15] A. Huck, G. Klotz, A. Knipper, C. Miehé, C. Richard-Serre, G. Walter, A. Poves, H. L. Ravn, and G. Marguier, *Phys. Rev. C* **31**, 2226 (1985).
- [16] A. Gade *et al.*, *Phys. Rev. C* **74**, 021302(R) (2006).
- [17] R. V. F. Janssens *et al.*, *Phys. Lett. B* **546**, 55 (2002).
- [18] D.-C. Dinca *et al.*, *Phys. Rev. C* **71**, 041302(R) (2005).
- [19] J. I. Prisciandaro *et al.*, *Phys. Lett. B* **510**, 17 (2001).
- [20] A. Bürger *et al.*, *Phys. Lett. B* **622**, 29 (2005).
- [21] F. Wienholtz *et al.*, *Nature (London)* **498**, 346 (2013).
- [22] M. Rosenbusch *et al.*, *Phys. Rev. Lett.* **114**, 202501 (2015).
- [23] T. Otsuka, R. Fujimoto, Y. Utsuno, B. A. Brown, M. Honma, and T. Mizusaki, *Phys. Rev. Lett.* **87**, 082502 (2001).
- [24] M. Honma, T. Otsuka, B. A. Brown, and T. Mizusaki, *Phys. Rev. C* **65**, 061301(R) (2002).
- [25] S. N. Liddick *et al.*, *Phys. Rev. Lett.* **92**, 072502 (2004).
- [26] D. Steppenbeck *et al.*, *Nature (London)* **502**, 207 (2013).
- [27] J. D. Holt, T. Otsuka, A. Schwenk, and T. Suzuki, *J. Phys. G* **39**, 085111 (2012).
- [28] G. Hagen, M. Hjorth-Jensen, G. R. Jansen, R. Machleidt, and T. Papenbrock, *Phys. Rev. Lett.* **109**, 032502 (2012).
- [29] A. T. Gallant *et al.*, *Phys. Rev. Lett.* **109**, 032506 (2012).
- [30] T. Otsuka and T. Suzuki, *Few-Body Syst.* **54**, 891 (2013).
- [31] J. D. Holt, J. Menéndez, and A. Schwenk, *J. Phys. G* **40**, 075105 (2013).
- [32] J. D. Holt, J. Menéndez, J. Simonis, and A. Schwenk, *Phys. Rev. C* **90**, 024312 (2014).
- [33] T. Otsuka, T. Suzuki, R. Fujimoto, H. Grawe, and Y. Akaishi, *Phys. Rev. Lett.* **95**, 232502 (2005).
- [34] W. Mayer, K. E. Rehm, H. J. Körner, W. Mayer, E. Müller, I. Oelrich, H. J. Scheerer, R. E. Segel, P. Sperr, and W. Wagner, *Phys. Rev. C* **22**, 2449 (1980).
- [35] <http://www.nndc.bnl.gov/>.
- [36] H. Scheit *et al.*, *Phys. Rev. Lett.* **77**, 3967 (1996).
- [37] A. Gade *et al.*, *Phys. Rev. C* **68**, 014302 (2003).
- [38] S. Calinescu *et al.*, *Acta Phys. Pol. B* **45**, 199 (2014).
- [39] D. Mengoni *et al.*, *Phys. Rev. C* **82**, 024308 (2010).
- [40] Z. P. Li, J. M. Yao, D. Vretenar, T. Nikšić, H. Chen, and J. Meng, *Phys. Rev. C* **84**, 054304 (2011).
- [41] E. Caurier, F. Nowacki, and A. Poves, *Eur. Phys. J. A* **15**, 145 (2002).
- [42] E. Caurier, F. Nowacki, and A. Poves, *Nucl. Phys. A* **742**, 14 (2004).
- [43] R. Winkler *et al.*, *Phys. Rev. Lett.* **108**, 182501 (2012).
- [44] T. Glasmacher *et al.*, *Phys. Lett. B* **395**, 163 (1997).
- [45] D. Sohler *et al.*, *Phys. Rev. C* **66**, 054302 (2002).
- [46] C. Force *et al.*, *Phys. Rev. Lett.* **105**, 102501 (2010).
- [47] D. Santiago-Gonzalez *et al.*, *Phys. Rev. C* **83**, 061305(R) (2011).
- [48] Z. Meisel *et al.*, *Phys. Rev. Lett.* **114**, 022501 (2015).
- [49] Zs. Dombrádi *et al.*, *Nucl. Phys. A* **727**, 195 (2003).
- [50] L. A. Riley *et al.*, *Phys. Rev. C* **72**, 024311 (2005).
- [51] S. Bhattacharyya *et al.*, *Phys. Rev. Lett.* **101**, 032501 (2008).
- [52] A. Gade *et al.*, *Phys. Rev. Lett.* **102**, 182502 (2009).
- [53] D. Steppenbeck *et al.* JPS Conf. Proc. (to be published).
- [54] L. Weissman *et al.*, *Phys. Rev. C* **67**, 054314 (2003).
- [55] T. Ohnishi *et al.*, *J. Phys. Soc. Jpn.* **77**, 083201 (2008).
- [56] T. Kubo *et al.*, *Prog. Theor. Exp. Phys.* **2012**, 03C003 (2012).

- [57] S. Takeuchi, T. Motobayashi, Y. Togano, M. Matsushita, N. Aoi, K. Demichi, H. Hasegawa, and H. Murakami, *Nucl. Instrum. Methods Phys. Res., Sect. A* **763**, 596 (2014).
- [58] P. Doornenbal *et al.*, *Phys. Rev. Lett.* **103**, 032501 (2009).
- [59] P. Doornenbal *et al.*, *Phys. Rev. Lett.* **111**, 212502 (2013).
- [60] S. Agostinelli *et al.* (GEANT4 Collaboration), *Nucl. Instrum. Methods Phys. Res., Sect. A* **506**, 250 (2003).
- [61] J. Papuga *et al.*, *Phys. Rev. Lett.* **110**, 172503 (2013).
- [62] Y. Utsuno, T. Otsuka, Y. Tsunoda, N. Shimizu, M. Honma, T. Togashi, and T. Mizusaki, [arXiv:1409.4506](https://arxiv.org/abs/1409.4506); JPS Conf. Proc. (to be published).
- [63] Y. Utsuno *et al.* (to be published).
- [64] N. Shimizu, [arXiv:1310.5431](https://arxiv.org/abs/1310.5431).
- [65] L. Gaudefroy *et al.*, *Phys. Rev. Lett.* **97**, 092501 (2006).
- [66] A. Signoracci and B. A. Brown, *Phys. Rev. Lett.* **99**, 099201 (2007).